

Preparation and Characterization of Biodegradable Electrospun Polyanhydride Nano/Microfibers

Qiuxiang Su, Aijun Zhao, Hongsen Peng, and Shaobing Zhou*

School of Materials Science and Engineering, Key Laboratory of Advanced Technologies of Materials, Ministry of Education, Southwest Jiaotong University, Chengdu, 610031, P. R. China

The biodegradable polyanhydride copolymers P(CPP–SA) composed of *p*-carboxybenzoic acid (CPP) and sebacic acid (SA) at weight ratios of 20:80, 35:65 and 50:50 were polymerized by a melt polycondensation process without catalyst. The copolymers were characterized by fourier transform infrared spectroscopy (FT-IR), ¹H-nuclear magnetic resonance (¹H-NMR), Ubbelohde viscometer, differential scanning calorimetry (DSC) and wide angle X-ray powder-diffraction (XRD). P(CPP–SA) nano/microfibers were the first time to be fabricated by electrospinning. The copolymers hold an excellent fibre-forming performance and the diameter range of 80–3,200 nm can be obtained. The *in vitro* degradation of the polyanhydride copolymers was evaluated in form of the nano/microfibers by investigating the change of fibrous morphology, weight loss and pH change of degradation medium. The experimental results showed that degradation rate was fast in the first day and slow in the following period, furthermore the degradation rate decreased with the increase of the content of CPP in copolymers. Therefore, the electrospun polyanhydride nano/microfibers exhibited strong potential as drug delivery vehicle and tissue engineering scaffold.

Keywords: Polyanhydride, X-ray Diffraction, Ultrafine, Fibers, Degradation.

1. INTRODUCTION

Polyanhydrides as a new class of biodegradable polymers have been developed since 1980s' by the group of Langer,¹ which now have been used widely in a number of applications for controlled release devices for drugs treating anticancer agents,^{2,3} local anesthetics,⁴ chemotherapeutic agents,^{5,6} anticoagulants,⁷ peptides and protein therapeutic.^{8–11} Based on the outlined advantage of degradable polymers there have been numerous polymers explored, while polyanhydrides can be used widely in biomedical field for good biocompatibility and variable degradation properties. Compared with the bulk erosion process of polylactide (PLA) and polylactide-co-glycolide (PLGA),^{12–14} polyanhydrides are believed to predominantly undergo surface erosion which is also termed heterogeneous erosion for hydrolytic instability of the anhydride bond and hydrophobicity.^{15–17} The outer drug can be released by steady speed from the polymers and the inner drug has been protected from biological environment throughout the surface erosion process, which made polyanhydride have particular advantages as drug delivery carriers.¹⁸ Polyanhydrides are most commonly prepared by

the melt polycondensation method as reported by Hill and Carothers.^{19,20} Since polyanhydrides with high molecular weight have been often obtained by melt polycondensation compared to other methods such as interfacial condensation, dehydrative coupling agents, solution polymerization and so on.^{21–27}

Polymer processing techniques are being explored for the incorporation of drug molecules into delivery vehicles of various geometries. As framework controlled release polymer, sustained-release wafers, beads and microspheres using polyanhydrides loaded with appropriate drug can be prepared by relevant processing techniques in previous research.^{3,28–31} While in our study, we choose polyanhydride nano/microfibers for controlled release device, which have not been reported yet. The main advantages of polyanhydrides nano/microfibers are as follows. Firstly, they have excellent fiber forming property.³² Secondly, the locally delivery and controlled release profiles make electrospun nano/microfibers potential as implantable drug carriers and functional coating of medical devices. The very large surface area to volume ratio, flexibility in surface functionalities, superior mechanical performance, and versatility of design are some of the characteristics that make the polymer nanofibers optimal candidates for many important applications.^{33,34} Therefore, we can anticipate

*Authors to whom correspondence should be addressed.

that the nano/microfibers have potential in drug controlled release system.

In this study, we synthesized biodegradable poly-anhydrides composed of sebacic acid (SA) and 1, 3-bis (p-carboxyphenoxy) propane (CPP) via melt polycondensation. The copolymers were characterized by FT-IR, ¹H-NMR, XRD, DSC and Ubbelohde viscosity technique. Polyanhydride nano/microfibers were also fabricated using electrospinning, since it is one of the few techniques to prepare long fibers with nano- to micrometer diameter.^{33, 35–44} The *in vitro* degradation of polyanhydride nano/microfibers was further studied.

2. MATERIALS AND METHODS

2.1. Materials

Sebacic acid was recrystallized three times from ethanol. Acetic anhydride was distilled from magnesium. 1, 3-Dibromopropane, *p*-hydroxybenzoic acid and all other solvents were used as received without further purification. All the other chemicals were analytical reagent grade.

2.2. Characterization

Infrared spectra were obtained using a Nicolet 5700 spectrometer. The samples were pressed into KBr pellets for analysis. ¹H-NMR spectra were obtained on a Bruker AM 300 apparatus using CDCl₃ as a solvent and TMS as an internal reference. Intrinsic viscosity ($[\eta]$) of polymers was measured in a chloroform solution (polymer concentration 1% w/v) at 23 °C using a Ubbelohde viscometer. The thermal properties of polymer were determined by differential scanning calorimetry (DSC) (Netzsch STA 449 C, Bavaria, Germany) from room temperature to 300 °C with a heating rate of 10 °C/min under a nitrogen atmosphere. The crystallinity of copolymer was characterized using an X-ray diffractometer (XRD) (Philips, X'Pert PRO, Netherlands) and scanning was done in the 2 θ angle range of 5–45°. The morphology of the polyanhydride fibers was investigated by using scanning electron microscope (SEM) (FEI, Quanta200, America) equipped with field-emission gun (10 kV) and robinson detector after 2 min of gold coating to minimize a charging effect.

2.3. The Synthesis of P(CPP-SA) Copolymers

2.3.1. Preparation of *p*-Carboxyphenoxy Propane

Prewighted sodium hydroxide, *p*-hydroxybenzoic and distilled water were added into a three-necked flask equipped with mechanical stirrer, reflux condenser and dropping funnel. The mixture was heated at reflux and 1, 3-Dibromopropane was dropped into for 1 h, followed by keeping on reflux for 5 h. Then sodium hydroxide water

solution was added into and refluxed again for 1 h, and the obtained solution was stirred to receive white precipitate. After filtration the collection was washed with anhydrous ethanol. The residue was dissolved in water, extracted with dried ether and neutralized with 6NH₂SO₄. After washing with water and drying in vacuum, CPP product was obtained. Its yield was about 50%. ¹H-NMR (CDCl₃): δ 12.54 (s, COOH), 7.87, 7.04 (d, 4H, ArH), 4.21 (t, 4H, CH₂O), 2.21 (m, 2H, CH₂). IR (KBr, cm⁻¹): 2954, 2889 (CH₂), 1693 (C=O).

2.3.2. Preparation of Acylated Prepolymers

Prewighted sebacic acid was refluxed in acetic anhydride for 1 h under nitrogen atmosphere and excess acetic anhydride was removed by drying under vacuum at 65 °C. The crude prepolymer was recrystallized from dried toluene. The crystals were washed with the mixed solvent of dried ether and petroleum ether (*v/v* = 50/50) to remove traces of acetic anhydride and toluene. Then, the final products were dried under vacuum. Its yield was about 87%. ¹H-NMR (CDCl₃): δ 2.46 (t, 4H, C(=O)CH₂), 1.67 (m, 4H, CH₂), 1.31 (m, 8H, CH₂). IR (KBr, cm⁻¹): 1806, 1740 (anhydride C=O).

Prewighted CPP was refluxed in 100 mL acetic anhydride for 25 min under nitrogen atmosphere and then, unreacted diacid was removed by filtration. The CPP prepolymer was deposited with dry ethyl ether at 0 °C and dried under vacuum. Its yield was about 79%. ¹H-NMR (CDCl₃): δ 7.99, 7.12 (d, 4H, Ar-H), 4.26 (t, 4H, CH₂O), 2.35 (s, 6H, CH₃), 2.27 (m, 2H, CH₂). IR (KBr, cm⁻¹): 1801, 1720 (anhydride C=O).

2.3.3. Preparation of Copolymer

CPP prepolymer and SA prepolymer were mixed in defined ratio in a three-necked flask under nitrogen. The flask was immersed in an oil bath and the prepolymers were allowed to melt after reaching 180 °C, and then, the pressure was reduced to 50~60 mmHg. The acetic anhydride condensed as byproduct was collected in a liquid nitrogen trap. After a defined time, the crude polymer was allowed to cool, dissolved in dichloroformethane, precipitated in petroleum ether. The precipitate was then washed with anhydrous ether and dried under vacuum at room temperature. The polymers obtained were stored at -20 °C. ¹H-NMR (CDCl₃): δ 7.98, 6.95 (d, ArH), 4.25 (t, CH₂O), 2.44 (t, C(=O)CH₂), 2.33 (m, CH₂), 1.64 (m, CH₂), 1.31 (m, CH₂). IR (KBr, cm⁻¹): 1810, 1740, 1720 (anhydride C=O).

2.4. Preparation of Polyanhydride Nano/Microfibers

The electrospinning apparatus was equipped with a high-voltage statitron (Tianjing High Voltage Power Supply Co.,

Tianjing, China). The copolymer was dissolved in chloroform solvent and then added in a 5 mL syringe attached to a circular-shaped metal capillary. The circular orifice of the capillary has an inner diameter of 0.6 mm. An oblong counter electrode is located about 15–18 cm from the capillary tip. The flow rate of the polymer and drug solution was controlled within 1 mL/h by a precision pump (Zhejiang University Medical Instrument Co., Hangzhou, China) to maintain a steady flow from the capillary outlet. The applied voltage was controlled within the range 15–20 kV.⁴⁷

2.5. Degradation of Polyanhydride Nano/Microfibers

80 mg of P(CPP–SA) nano/microfibers was placed individually in test tube containing 10 mL of 0.1 M phosphate-buffered saline (PBS) at pH 7.4. The tubes were kept in a thermo-stated incubator (Haerbin Dongming Medical Equipment Company) which was maintained at 37 °C and 100 cycles/min. At predetermined time intervals, the remaining fibers were collected by centrifugation, washed with distilled water and freeze-dried. Samples then weighed to determine the weight loss due to degradation of copolymer. The pH values of the degradation medium were measured using an Orion pH meter with a pH glass electrode. The meter was calibrated using KCl standard solutions.

3. RESULTS AND DISCUSSION

3.1. Polyanhydride Synthesis

The polyanhydrides were synthesized in a melt polycondensation process in accordance with the protocol established by Domb et al.²¹ Firstly, aromatic monomer CPP monomer was synthesized with *p*-hydroxybenzoic acid and 1, 3-dibromopropane. Later, acetic mixed anhydride prepolymers were prepared by heating corresponding diacids in acetic anhydride. Finally, P(CPP–SA) copolymers with CPP/SA weight ratios of 20:80, 35:65 and 50:50 were synthesized by melt-polycondensation of CPP prepolymer and SA prepolymer. Table I summarizes the properties of P(CPP–SA) copolymers with different ratios of CPP and SA. From DSC data, we can find that the melting temperature (T_m) of these copolymers was almost similar when CPP content is below 35 wt%, but there was a

sharp rise in T_m as the CPP content increased to 50 wt%. The result is in agreement with previous report.⁴⁶ Based on the literature, we can know that melting point of SA and CPP homopolymers is 86 and 240 °C, respectively. When CPP content in copolymer is near 50 wt%, its melting point will be gradually close to T_m of CPP homopolymer. The factual weight percentages of SA and CPP in the copolymers were in good agreement with the feed ratio. The amount of SA in the copolymer was slightly higher than the amount fed, while the CPP amount was slightly less than fed. Furthermore, the molecular weight decreases with increasing CPP content in the same experimental conditions. The reason is that aromatic acid has lower reactivity than aliphatic acid. Reactivity decreases with increased the CPP amount, which results in depressing chain interactions with CPP in polymerization, and subsequently reducing the content of CPP, the molecular weight of polyanhydride increases.

3.2. Fourier Transform Infrared Spectra (FT-IR)

FT-IR spectra of P(CPP–SA) copolymers show typical three characteristic anhydride carbonyl peaks at 1810, 1740 and 1720 cm^{-1} , the C–H stretching vibrations of long aliphatic alkyl at 2900 and 2850 cm^{-1} , and the C–O stretching of anhydride group at 1070 cm^{-1} and 1040 cm^{-1} (see Fig. 1). With the amount of CPP in the copolymer increasing the intensity of peaks at 1720 cm^{-1} also increased while the intensity of the peak at 1740 cm^{-1} decreased.

3.3. Nuclear Magnetic Resonance (NMR)

Figure 2 shows the ¹H-NMR spectrum of P(CPP–SA) copolymer obtained by melt polycondensation. The well resolved chemical shifts at $\delta = 1.3, 1.6,$ and 2.4 ppm belong to the hydrogen atoms of individual functional groups on poly(sebacic anhydride) and chemical shifts at 2.33, 4.25, 6.95, and 7.98 ppm ascribed to the protons of CPP. The peak at 7.25 ppm corresponds to the d-chloroform. The spectrum also confirmed that the polyanhydrides were provided with anticipated structure. The actual weight percentages of SA and CPP in the polymer were estimated by integration and comparison of the corresponding NMR peaks, which were in good agreement with the monomer feed ratios, also as shown in Table I.

Table I. Characterization of P(CPP–SA) copolymers.

CPP:SA in the feed (wt%)	CPP:SA ¹ H-NMR (wt%) ^a	Yield (%)	Intrinsic viscosity ($[\eta]$) ^b	Viscosity weight average ^c	T_m (°C) ^d	Crystallinity (%) ^e
20:80	17.8:82.2	82	0.3805	35187	63.6	37.9
35:65	33.5:66.5	76	0.2441	17922	57.5	28.8
50:50	43.6:56.4	58	0.2154	14819	185.1	16.2

^aCalculated by ¹H-NMR. ^bDetermined using a Ubbelohde viscometer at 23 °C. ^cCalculated by the formula as follow.¹⁸ $[\eta]_{\text{CHCl}_3}^{296\text{K}} = 3.88 \times 10^{-4} \text{M}^{0.658}$. ^dDetermined by DSC. ^eCalculated using XRD.

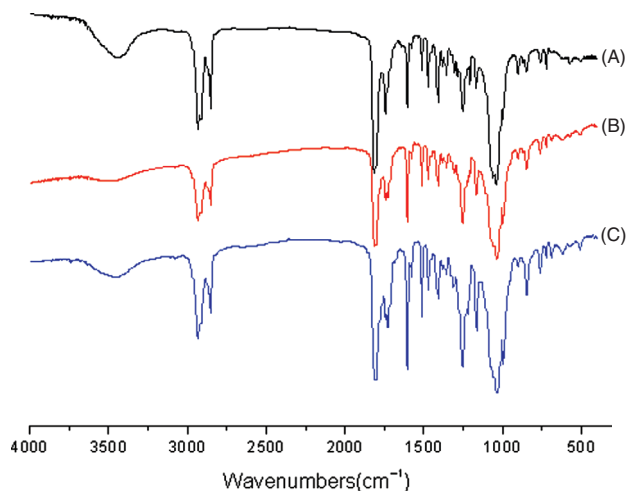


Fig. 1. FT-IR spectra of P(CPP-SA) (A) 20:80; (B) 35:65; (C) 50:50.

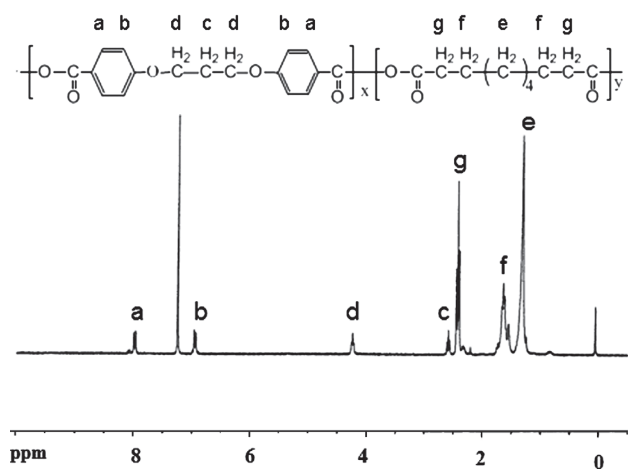


Fig. 2. $^1\text{H-NMR}$ spectra of 20:80 P(CPP-SA) copolymer.

3.4. X-ray Diffraction (XRD)

For degradable polymers, the erosion behavior is based on the polymer microstructure which is composed of amorphous and crystalline polymer parts, and the amorphous structures erode faster than crystalline ones. Therefore, crystallinity is an important factor that controls polymer

erosion. The crystallinity was determined by X-ray diffraction based the reported methods.^{48,49} In general, the peaks of amorphous and crystalline overlap each other partially or fully for the crystalline polymers. Therefore, it is important to realize that distinguishing between the two different types of peaks is a very meaningful work. The analysis method is derived from Gauss-Cauchy Compound function, which was put forward by Hindeleh etc.⁵⁰ to characterize the curve of X-ray diffraction. An amorphous intensity curve and multiple peaks separation program based on XRD pattern were employed (Fig. 3). The degree of crystallinity calculated from the pattern was shown in Table I. The data show that the crystallinity of polyanhydride reduces to the low-water mark while the monomer content of CPP/SA tends to 1:1, which may lead to an increase in the confusion degree and a decline in the structural regularity. Thus, it further resulted in the depression of the degree of crystallinity.

3.5. Degradation of P(CPP-SA) Ultrafine Fibers

After P(CPP-SA) copolymers were dissolved in methylene chloride solvent, the nano/microfibers were prepared by electrospinning. Figures 4(a, b and c) show original fibrous morphology of P(CPP-SA) copolymers observed by SEM. There was no obvious change on fibrous morphology of the copolymers with different CPP/SA weight ratios. P(CPP-SA) copolymers have good fibre-forming performance, and the nano/microfibers are straightforward and have smooth external surfaces without visible nodes. The size distribution of the fibers before degradation is from 80 nm to 3200 nm. The average fiber diameter of P(CPP-SA) with CPP/SA weight ratios of 20:80, 35:65 and 50:50 is 1030 ± 380 nm, 1690 ± 670 nm and 1310 ± 360 nm shown in Figures 4(a, b and c), respectively. Consequently, from these results a conclusion can be made that the morphology and diameter of the fibers are not affected basically by the monomer ratios of copolymers.

Figure 5 shows the weight loss profiles of P(CPP-SA) copolymers with different monomer ratios. There are two phases through our investigation of degradation. For one thing, copolymers degrade rapidly in the first day and

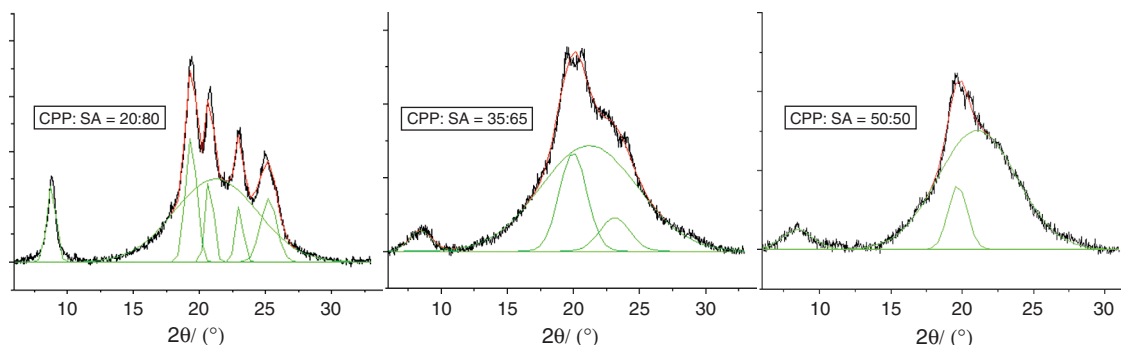


Fig. 3. Curve analysis of P(CPP-SA) X-ray diffraction.

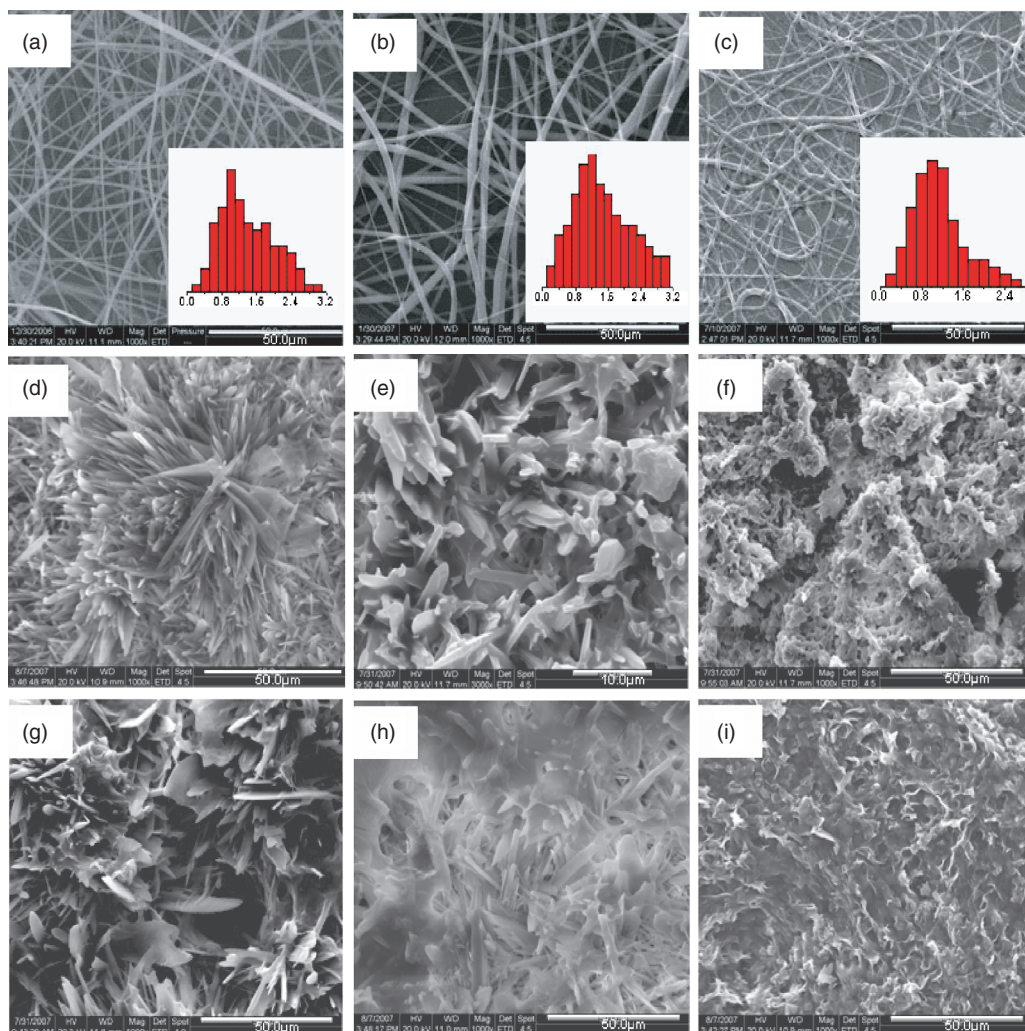


Fig. 4. SEM photos of 20:80 P(CPP-SA) after: (a) 0; (d) 7; (g) 13 d and 35:65 P(CPP-SA) after: (b) 0; (e) 7; (h) 13 d and 50:50 P(CPP-SA) after: (c) 0; (f) 1; (i) 13 d degradation in PBS at 37 °C.

weight loss up to 50%, which may be strongly related to their geometry and the composing of copolymer. Due to high specific surface area and porous structure of polyanhydride ultrafine fibers, the progress of degradation can be accelerated. Furthermore, in the first phase, SA segments would be prior to degrade compared with CPP segments owing to more hydrophilic for SA than CPP. And in the following period, the degradation presented slow-motion moment. The degradation rate is dependent on the content of CPP monomer, slower degradation rate were observed for more CPP content. The weight percentage of residue after 13 days was almost equal to the corresponding content of CPP in copolymers in all cases, which further suggested that the monomer CPP ratio in copolymer can affect the degradation rate.

For the *in vitro* degradation study, the nano/microfibers were degraded in PBS (pH 7.4) at 37 °C for 13 days. SEM photos show that the surface morphology of P(CPP-SA) fibers with CPP/SA ratios of 20:80, 35:65 and 50:50 changed during the degradation. To the best our knowledge

it was the first time to directly observe the degradation process. Compared with SEM photos in Figures 4(d–f), we can see that there were almost no fibers and only some sheet residue for 20:80 P(CPP-SA), but for 35:65 P(CPP-SA) and especially for 50:50 P(CPP-SA) some short fibers could be found. After 13 days' degradation, only sheet residue could be observed for all copolymers (Figs. 4(g–i)). Especially for 80:20 P(CPP-SA) copolymer, the outermost layer of fibers was first peeling off during degradation, which caused the diameter of internal layer become thinner. On the contrary, some layer peeled off exhibited bigger owing to the perimeter of outside layer of the fibers as shown in Figures 4(d and g). The phenomenon is similar to that cortex desquamated from a tree trunk. It indicated that the degradation occurred on fibers surface first. The degradation mechanism belonged to surface erosion. The results further confirmed that the degradation rate of the copolymer decreased with CPP content increasing. It is well known that during the degradation the weight of biodegradable polymers would lose because

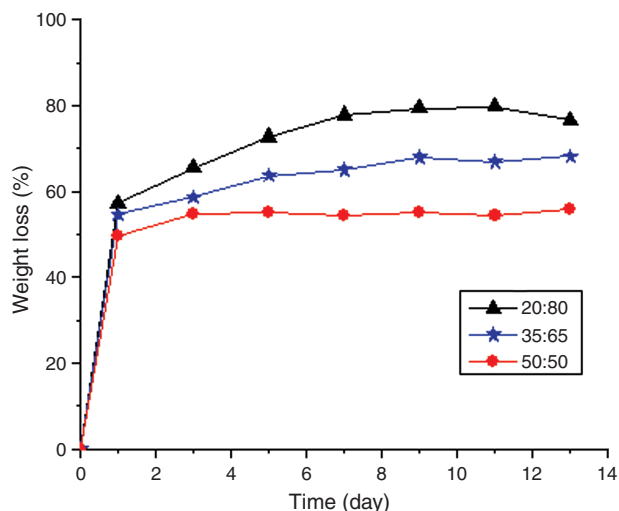


Fig. 5. Weight loss of 20:80, 35:65, 50:50 P(CPP-SA) nano/microfibers incubated in PBS at 37 °C.

their some degradation product dissolved in degradation medium. For P(CPP-SA) copolymers, their degradation products, only SA can be dissolved in water. It also indicated that the component of the sheet residue was mainly CPP, which could also be proved by the weight loss profiles in Figure 5. The mass of fibers decreased sharply in the initial 1 day, and then, only a slight mass loss was observed in the following period. Degradation of the polymer designates the process of a polymer chain cleavage, while erosion is the sum of all processes that lead to mass loss from polyanhydride matrix.⁵¹ The mass loss of fibers in the initial phase might result from low molecular weight part of copolymer dissolving into the degradation media and the cleaving of the more labile SA-SA bonds. In the following phase, the mass loss may be due to the hydrolysis of high molecule weight copolymer into oligomers or monomers.⁵² The XRD patterns of the residue were almost similar with that of PCPP homopolymer,⁴⁶ which further suggested that the residue was mainly low molecular weight PCPP and CPP crystals.

There are three kinds of bonds in P(CPP-SA) copolymers: SA-SA bonds, CPP-CPP bonds and SA-CPP bonds. David et al. reported that the following order of anhydride bond lability was determined: SA-SA \approx SA-CPP \gg CPP-CPP by using solution-state ¹H-NMR spectroscopy,²⁶ leading to preferential hydrolysis of aliphatic blocks within the copolymer chain. Therefore, the more CPP content, the more CPP-CPP bonds in polyanhydride copolymer and the slower degradation rate, which is consistent with the experimental results (Figs. 4–6).

The pH values of the degradation medium were also measured to investigate the degradable property of the copolymer as shown in Figure 6. P(CPP-SA) degraded into CPP and SA monomers, which diffused into degradation medium resulted in pH decrease. The pH change profiles were similar with weight loss change. The reason is same as above description.

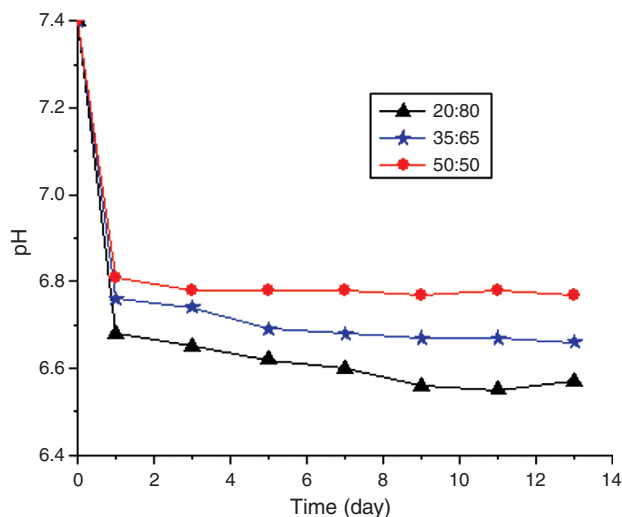


Fig. 6. The pH change of medium for 20:80, 35:65, 50:50 P(CPP-SA) nano/microfibers incubated in PBS at 37 °C.

4. SUMMARY

The copolymers of CPP and SA can be synthesized by melt polycondensation without any catalyzer. The polymers with anticipant structure were proven by FT-IR and ¹H-NMR analysis. The crystallinity of P(CPP-SA) copolymers was in reverse to the content of CPP from the investigation. In order to widen biomedical application of the polymer, we successfully prepared P(CPP-SA) nano/microfibers by electrospinning for the first time to the best of our knowledge. The fibers exhibited an excellent fibre-forming performance. The *in vitro* degradation of P(CPP-SA) nano/microfibers showed two phases: near 50% fast degradation in the first day and followed gradual degradation and furthermore the rate decreased with CPP component increase. The degradation rate can be controlled by adjusting the molar ratios of CPP and SA. Therefore, P(CPP-SA) may be potential in form of fiber for biomedical application as drug controlled release carrier and tissue engineering scaffold.

Acknowledgments: This work was partially supported by National Natural Science Foundation of China (50773065, 30970723), Programs for New Century Excellent Talents in university, Ministry of Education of China (NCET-07-0719) and Sichuan Prominent Young Talent Program (08ZQ026-040).

References and Notes

1. H. B. Rosen, J. Chang, G. E. Wnek, R. J. Linhardt, and R. Langer, *Biomaterials* **4**, 131 (1983).
2. J. M. Gao, L. Niklason, X. M. Zhao, and R. Langer, *J. Pharm. Sci.* **87**, 246 (1998)
3. M. S. Kim, K. S. Seo, H. S. Seong, S. H. Cho, H. B. Lee, K. D. Hong, S. K. Kim, and G. Khan, *Bio-Med. Mater. Eng.* **15**, 229 (2005).

4. D. B. Masters, C. B. Berde, S. Dutta, T. Turek, and R. Langer, *Pharm. Res.* 10, 1527 (1993).
5. C. L. Nelson, S. O. Hickmon, and R. A. Skinner, *J. Orthop. Res.* 15, 249 (1997).
6. C. Wu, J. Fu, and Y. Zhao, *Macromolecules* 33, 9040 (2000).
7. D. Chickering, J. Jacob, and E. Mathiowitz, *Biotechnol. Bioenerg.* 52, 96 (1996).
8. K. E. Uhrich, S. M. Cannizzaro, R. S. Langer, and K. M. Shakesheff, *Chem. Rev.* 99, 3181 (1999).
9. A. S. Determan, J. H. Wilson, and M. J. Kipper, *Biomaterials* 27, 3312 (2006).
10. M. P. Torres, A. S. Determan, and G. L. Anderson, *Biomaterials* 28, 108 (2007).
11. H. L. Jiang and K. J. Zhu, *Int. J. Pharm.* 194, 51 (2000).
12. H. Gollwitzer, K. Ibrahim, H. Meyer, W. Mittelmeier, R. Busch, A. Stemberger, and J. Antimicrob, *Chemother.* 51, 585 (2003).
13. P. Caliceti and S. Salmaso, *J. Control. Release* 94, 195 (2004).
14. H. Seong, D. Moon, G. Khang, and H. B. Lee, *Polymer* 26, 128 (2002).
15. A. Göpferich and J. Tessmar, *Adv. Drug Deliver. Rev.* 54, 911 (2002).
16. F. Burkeros, L. Schedlb, and A. G. Opferich, *Biomaterials* 23, 4221 (2002).
17. J. P. Jaina, S. Modia, and A. J. Domb, *J. Control. Release* 103, 541 (2005).
18. N. Kumar, R. S. Langer, and A. J. Domb, *Adv. Drug Deliver. Rev.* 54, 889 (2002).
19. J. W. Hill, *J. Am. Chem. Soc.* 52, 4110 (1930).
20. J. W. Hill and H. W. Carothers, *J. Am. Chem. Soc.* 54, 5169 (1932).
21. A. J. Domb and R. Langer, *J. Polym. Sci., Part A* 25, 3373 (1987).
22. A. J. Domb, S. Amselem, J. Shah, and M. Maniar, *Adv. Polym. Sci.* 107, 93 (1993).
23. W. C. Lee and I. M. Chu, *J. Biomed. Mater. Res. B Appl Biomater* 84, 138 (2008).
24. S. Hou, L. K. McCauley, and P. X. Ma, *Macromol. Biosci.* 7, 620 (2007).
25. J. Fu, J. Fiegel, and J. Hanes, *Macromolecules* 37, 7174 (2004).
26. D. L. McCann, F. Heatley, and A. D'Emanuele, *Polymer* 40, 2151 (1999).
27. R. J. Tamargo, J. I. Epstein, C. S. Reinhard, M. Chasin, and B.-H. Bren, *J. Biomed. Mater. Res.* 23, 253 (1989).
28. W. X. Guo, K. X. Huang, R. Tang, and Q. Chi, *Polymer* 45, 5743 (2004).
29. D. Stephens, L. Li, D. Robinson, S. Chen, H. Chang, R. M. Liu, Y. Tian, E. J. Ginsburg, X. Gao, and T. Stultz, *J. Control. Release.* 63, 305 (2000).
30. C. A. Santos, B. D. Freedman, K. J. Leach, D. L. Press, M. Scarpulla, and E. Mathiowitz, *J. Control. Release* 60, 11 (1999).
31. M. J. Kipper, E. Shenb, and A. Determan, *Biomaterials* 23, 4405 (2002).
32. A. Conix, *J. Polym. Sci. Part A.* 29, 343 (1958).
33. S. Zhou, H. Peng, X. Yu, X. Zheng, W. Cui, Z. Zhang, X. Li, J. Wang, J. Weng, W. Jia, and F. Li, *J. Phys. Chem. B.* 112, 11209 (2008).
34. P. Gibson and G. H. Schreuder, *Journal of Coated Fabrics* 28, 63 (1998).
35. J. Zeng, X. Y. Xu, and X. S. Chen, *J. Control Release* 92, 227 (2003).
36. D. S. Katti, K. W. Robinson, F. K. Ko, and C. T. Laurencin, *J. Biomed. Mater. Res. Part B: Appl Biomater.* 70B, 286 (2004).
37. K. P. Rajesh and T. S. Natarajan, *J. Nanosci. Nanotechnol.* 9, 5402 (2009).
38. P. Tyagi, S. Catledge, A. Stanishevsky, V. Thomas, and Y. K. Vohra, *J. Nanosci. Nanotechnol.* 9, 4839 (2009).
39. J. A. Lopes-da-Silva, B. Veleirinho, and I. Delgadillo, *J. Nanosci. Nanotechnol.* 9, 3798 (2009).
40. Z. Han, H. Kong, J. Meng, C. Wang, S. Xie, and H. Xu, *J. Nanosci. Nanotechnol.* 9, 1400 (2009).
41. H. Y. Wang, Y. Yang, Y. Wang, Y. Y. Zhao, X. Li, and C. Wang, *J. Nanosci. Nanotechnol.* 9, 1522 (2009).
42. X. Xu, Qi. Yang, J. Bai, T. Lu, Y. Li, and X. Jing, *J. Nanosci. Nanotechnol.* 8, 5066 (2008).
43. S. Roh, Y. Lee, J. Lee, and S. Kim, *J. Nanosci. Nanotechnol.* 8, 5147 (2008).
44. Y. Liu, S. Sagi, R. Chandrasekar, L. Zhang, N. Hedin, and H. Fong, *J. Nanosci. Nanotechnol.* 8, 1528 (2008).
45. E. Hempel, J. Lindau, U. Rotz, H. Fischer, H. Utschick, and F. Kuschel, *Mol. Cryst and Liq. Cryst.* 193, 199 (1990).
46. E. Mathiowitz, E. Ron, G. Mathiowitz, C. Amato, and R. Langer, *Macromolecules.* 23, 3212 (1990).
47. H. Peng, S. Zhou, T. Guo, Y. Li, X. Li, J. Wang, and J. Weng, *Colloids Surf., B: Biointerfaces* 66, 206 (2008).
48. C. X. Ao, *Journal of Northwest University (Natural Science Edition)* 33, 9 (2003).
49. Z. S. Mo and H. F. Zhang, *Polym. Mater. Sci. Eng.* 3, 9 (1988).
50. A. M. Hindeleh and D. J. Johnson, *Polymer* 19, 27 (1978).
51. A. Göpferich, *Biomaterials.* 18, 397 (1997).
52. L. Sun, S. Zhou, W. Wang, Q. Su, X. Li, and J. Weng, *J. Mater. Sci.: Mater. Med.* 20, 2035 (2009).

Received: 28 June 2009. Accepted: 1 November 2009.